

---

# ON THE NATURE OF A NARROW ROTON ABSORPTION LINE IN THE SPECTRUM OF A DISK-SHAPED SHF RESONATOR

V.M. LOKTEV, M.D. TOMCHENKO

Bogolyubov Institute for Theoretical Physics, Nat. Acad. Sci. of Ukraine  
 (14b, Metrolohichna Str., Kyiv 03680, Ukraine; e-mail:  
*vloktev@bitp.kiev.ua; mtomchenko@bitp.kiev.ua*)

PACS 67.10.Hk  
 ©2011

---

We calculate the probability of the creation of a circular phonon (c-phonon) in He II by a c-photon of the resonator. It is shown that this probability has sharp maxima at frequencies, where the effective group velocity of the c-phonon is equal to zero; the density of states of c-phonons strongly grows at such frequencies. For He II, these frequencies correspond to a roton and a maxon. From the probability of the c-roton creation, we calculate the roton line width which is found to approximately agree with the experimental one. We conclude that the roton line observed in the super-high-frequency (SHF) absorption spectrum of helium is related to the creation of c-rotors. A possible interpretation of the Stark effect observed for the roton line is also proposed.

## 1. Introduction

In the recent works [1, 2], an unconventional effect was discovered. In a dielectric disk-shaped resonator placed in liquid  $^4\text{He}$ , the azimuth ( $l$ -)modes were excited. These modes are of the “whispering-gallery” type and represent a superposition of standing and running resonance electromagnetic (EM) waves of the SHF range in a narrow frequency interval. At the roton frequency  $\nu_{\text{rot}} = \Delta_{\text{rot}}/2\pi\hbar = 180.3$  GHz, the supernarrow absorption line with the width  $\Delta\nu \simeq 50$  kHz was observed in the SHF spectrum of the resonator. This width is by six orders less than that of a roton peak measured in neutron experiments and is comparable with the width of lines in the Mössbauer effect. It was assumed in [2] that the line is related to the Van Hove singularity caused by a high density of states of plane (p-) rotors near the roton minimum of the dispersion curve. In this case, however, one is faced with the problem to satisfy the momentum conservation law, since the p-roton momentum is greater than the momentum of a p-photon with the same energy by six orders. Therefore, it was supposed [2] that the excess momentum of a p-roton is transferred to helium as a whole.

To clarify this and other points, it is necessary to calculate the probability of the creation of a roton and the

widths and the forms of lines for various possible processes, and then to choose a process explaining the experiment. It is necessary to take into account that the EM field of a disk-shaped resonator has the circular (c-) symmetry and is concentrated only near the disk according to measurements [1] and the theory [3]. Since namely the EM field induces the transition, the latter must be characterized by the c-symmetry. In [3], it was shown that a phonon near a disk possesses also the c-symmetry. Therefore, we assume that the narrow line corresponds to the creation of a c-roton by the EM field of the resonator. Below, we will find the probability of this process and the width of the corresponding absorption line.

A number of results required for calculations was obtained in [3]; formulas (N) from that work will be denoted here by (N\*). A part of the results of the present work was briefly published in [4].

## 2. Probability of the Creation of a Circular Phonon by the Field of a Resonator

To calculate the line width, it is necessary to know the probability of the c-photon  $\rightarrow$  c-phonon process. No problems concerning the conservation laws appear for this process, because both c-photon and c-phonon have no momentum, but have angular momenta  $L_z = \hbar l$  and  $L_z = \hbar l_c$ , respectively [3]. Moreover, the condition  $l = l_c$  is easily satisfied. As will be seen, the field of the resonator contains  $\sim 10^{12}$  photons with close frequencies. At such occupation number, the photon field can be considered as an external classical perturbing harmonic field with frequency  $\nu$  acting on helium. We now calculate the probability of the creation of a c-phonon by this field. The width of the azimuth mode, on which the roton line is observed, is about 2.5 MHz, the line width  $\sim 0.1$  MHz, and the frequency  $\nu = 180.3$  GHz. It is seen that the mode width is very small as compared with the

frequency; therefore, the latter can be considered constant.

It is worth noting that, while calculating the transition amplitude, we can take no care of the conservation laws. They are satisfied automatically (if a transition contradicts some conservation law, this will manifest itself in the disagreement of the symmetries of the initial and final states, and the amplitude will become equal to zero).

The probability (per unit time) of the creation of a c-phonon in He II due to the action of the EM field of a resonator is [5]

$$\delta w_{fi} = \frac{2\pi}{\hbar} |F_{fi}|^2 \delta(E_f - E_i^{(0)} - \hbar\omega), \quad (1)$$

$$F_{fi} = \int \Psi_f \hat{F} \Psi_i d\Omega^{\text{nuc}} d\Omega^{\text{el}}, \quad (2)$$

where  $d\Omega^{\text{nuc}} = d\mathbf{R}_1 \dots d\mathbf{R}_N$  and  $d\Omega^{\text{el}} = d\mathbf{R}_1^{(1)} d\mathbf{R}_1^{(2)} \dots d\mathbf{R}_N^{(1)} d\mathbf{R}_N^{(2)}$  are the phase volumes of all nuclei and all electrons,  $\Psi_i$  and  $\Psi_f$  are the wave functions (WFs) of the initial and final states of helium, respectively,  $E_f - E_i^{(0)} = E_c$  is the energy of a c-phonon, and  $\omega = 2\pi\nu$ . The explicit formula for  $\hat{F}$  follows from the perturbation operator

$$\hat{V} = \hat{F} e^{-i\omega t} + \hat{F}^\dagger e^{i\omega t}. \quad (3)$$

If the wavelength  $\lambda$  of the EM field is much more than the size of the system, then the problem is solved in the dipole approximation [6]. In our case, this approximation is not suitable, since the system size exceeds  $\lambda$  by one order. In addition, a photon is spent on the excitation of fluid helium as a whole, i.e. on the creation of a c-phonon which is related to the motion of atoms as united objects, rather than on the excitation of electron shells of a single atom or many atoms. Therefore, we will use a general approach, by considering the action of the EM field directly on the charged particles in an atom, i.e., on electrons and the nucleus. But the atoms interact with one another. As a result, the EM field creates the collective excitation, a phonon which is electrically neutral as a whole. It should be noted that a sound wave is associated with a variable concentration gradient. In this case, a variable local electric field arises in the interatomic space, since helium atoms polarize one another [7, 8]. However, this gives only a negligible correction to the effect. For a charged particle in the EM field, we have [5]

$$\hat{V} = -\frac{q}{2mc} (\mathbf{A}\hat{\mathbf{p}} + \hat{\mathbf{p}}\mathbf{A}) + \frac{q^2}{2mc^2} \mathbf{A}^2 =$$

$$= -\frac{q}{mc} \left( \mathbf{A}\hat{\mathbf{p}} - \frac{i\hbar}{2} \text{div}\mathbf{A} \right) + \frac{q^2 \mathbf{A}^2}{2mc^2}, \quad (4)$$

where  $\hat{\mathbf{p}} = -i\hbar\nabla_{\mathbf{r}}$ , and  $q$  and  $\mathbf{r}$  are the charge and the radius-vector of a particle, respectively. The term with  $\mathbf{A}^2$  induces two-photon transitions which will not be considered here. The field  $\mathbf{A}$  should be real and can be presented in the form

$$\mathbf{A}(\mathbf{r}, t) = \mathbf{A}_0(\mathbf{r})e^{-i\omega t} + \mathbf{A}_0^*(\mathbf{r})e^{i\omega t} + \tilde{\mathbf{A}}(\mathbf{r}). \quad (5)$$

The quantity  $\text{div}\mathbf{A}$  is calculated in [3], formula (6\*). Since we are interesting in the field  $\mathbf{A}$  in helium, we set  $\varepsilon_{\perp} = \varepsilon_z \equiv \varepsilon_h$  in (6\*). As a result, we obtain  $\text{div}\mathbf{A} = f_d(\mathbf{r})$ , i.e. the divergence is determined by the field  $\tilde{\mathbf{A}}(\mathbf{r})$ , i.e. the time-independent part of  $\mathbf{A}$ . It can be always set to zero, by adding a gradient of the corresponding function to  $\mathbf{A}$ . In this case, the measurable quantities  $\mathbf{E}$  and  $\mathbf{H}$  are not changed. Therefore, we set  $\tilde{\mathbf{A}}(\mathbf{r}) = 0$ , so that  $\text{div}\mathbf{A} = 0$ . In what follows, we omit index 0 in  $\mathbf{A}_0$  (5). So, we have

$$\hat{F} = \frac{i\hbar q}{mc} \mathbf{A}\nabla_{\mathbf{r}}. \quad (6)$$

Consider the set of He II atoms in the field  $\mathbf{A}$ . An atom of  ${}^4\text{He}$  consists of the nucleus with the charge  $q_n = -2e$  and two electrons, each possessing the charge  $q_e = e$ . Therefore, for He II, we have

$$\hat{F} = \sum_j \frac{i\hbar}{c} \left( \frac{q_n}{m_n} \mathbf{A}(\mathbf{R}_j) \frac{\partial}{\partial \mathbf{R}_j} + \frac{q_e}{m_e} \mathbf{A}(\mathbf{R}_j^{(1)}) \frac{\partial}{\partial \mathbf{R}_j^{(1)}} + \frac{q_e}{m_e} \mathbf{A}(\mathbf{R}_j^{(2)}) \frac{\partial}{\partial \mathbf{R}_j^{(2)}} \right). \quad (7)$$

Here,  $\mathbf{R}_j$  are coordinates of the nucleus of the  $j$ -th atom,  $\mathbf{R}_j^{(1)}$  and  $\mathbf{R}_j^{(2)}$  are coordinates of the electrons of this atom,  $m_n \approx m_4$  is the nucleus mass of  ${}^4\text{He}$  atom, and  $m_e$  is the electron mass.

To calculate  $F_{fi}$ , we need to know the WFs  $\Psi_f$  and  $\Psi_i$ . Let the initial state characterized by the WF  $\Psi_i$  be the ground state of helium, and let the final state with  $\Psi_f$  be the ground state plus one c-phonon. Then

$$\Psi_i \equiv \Psi_0(\{\mathbf{R}_j, \mathbf{R}_j^{(1,2)}\}) = \Psi_0^{\text{nuc}}(\{\mathbf{R}_j\}) \Psi_0^{\text{el}}(\{\mathbf{R}_j^{(1,2)}\}), \quad (8)$$

where  $\Psi_0^{\text{el}}$  is the WF of all electrons, and  $\Psi_0^{\text{nuc}}$  is the WF of all nuclei of helium atoms. The modern microscopic models describe the properties of He II well enough. According to them, a helium atom is a very elastic object.

Therefore, we can consider with a good accuracy that the electron shell of each atom follows the nucleus without inertia and is not deformed by the interaction with neighboring atoms. In this case,  $\Psi_0^{\text{nuc}}(\mathbf{R}_j)$  coincides with  $\Psi_0(\mathbf{R}_j)$  written as a function of the coordinates of atoms, and the electron part looks as

$$\begin{aligned} \Psi_0^{\text{el}} &= \prod_{j=1}^N \psi_j(\mathbf{R}_j^{(1)}, \mathbf{R}_j^{(2)}) \approx \prod_{j=1}^N \psi_{1s^2}(\mathbf{r}_j^{(1)}, \mathbf{r}_j^{(2)}) \approx \\ &\approx \prod_{j=1}^N \tilde{\psi}_{1s}(\mathbf{r}_j^{(1)}) \tilde{\psi}_{1s}(\mathbf{r}_j^{(2)}), \end{aligned} \quad (9)$$

where  $\mathbf{r}_j^{(1)} = \mathbf{R}_j^{(1)} - \mathbf{R}_j$ ,  $\mathbf{r}_j^{(2)} = \mathbf{R}_j^{(2)} - \mathbf{R}_j$ . For the WF of the ground state of  $^4\text{He}$  atom, we use the well-known one-parameter approximation with  $\tilde{\psi}_{1s}(\mathbf{r}) = \frac{1}{\sqrt{\pi a^3}} e^{-r/a}$  ( $a = 0.313 \text{ \AA}$ ). In reality, the electron shells of atoms are perturbed by neighbors and, as a result, are somewhat deformed [7, 8]. These deformations are “directed” to the atom, with which the interaction occurs. Since the adjacent atoms surround the given atom from all sides and chaotically on the average, the polarizations induced by them cancel one another to a significant degree. As a result, the mean polarization of an atom in He II turns out small,  $d \simeq 3 \times 10^{-4} |e| a_B$  [9], though it is greater by one order of magnitude than the polarization induced by a single atom located at the mean interatomic distance  $\bar{R} \approx 3.6 \text{ \AA}$ . The literature presents the assertions that the presence of large-amplitude zero oscillations of He II with the amplitude  $\sim \bar{R}$  implies that the electron shell of a helium atom is strongly deformed and “smeared” over several interatomic distances. However, this should not be accepted: zero oscillations mean only that, due to the strong interatomic interaction, the helium atoms move with a large (even at  $T = 0$ ) mean velocity, which leads to a small density of helium and exhausts the condensate. But the electron shells of atoms are deformed slightly in this case, as follows from the smallness of  $d$ . We will neglect these deformations and apply formula (9).

For the WF of a state with a single c-phonon, we use the formula [3]

$$\Psi_f = \Psi_0 \Psi_c(l_c, k_z, k_\rho). \quad (10)$$

In view of it, we obtain

$$\begin{aligned} F_{fi} &\approx \frac{2i\hbar|e|N}{cm_4} \int \Psi_0 \Psi_c^* \left( \mathbf{A}(\mathbf{R}_1) \frac{\partial}{\partial \mathbf{R}_1} - \right. \\ &\left. - \frac{m_4}{m_e} \mathbf{A}(\mathbf{R}_1^{(1)}) \frac{\partial}{\partial \mathbf{R}_1^{(1)}} \right) \Psi_0 d\Omega^{\text{nuc}} d\Omega^{\text{el}}. \end{aligned} \quad (11)$$

Let us take into account that

$$\frac{\partial \Psi_0}{\partial \mathbf{R}_1} = \Psi_0^{\text{el}} \frac{\partial \Psi_0^{\text{nuc}}}{\partial \mathbf{R}_1} + \Psi_0^{\text{nuc}} \frac{\partial \Psi_0^{\text{el}}}{\partial \mathbf{R}_1}, \quad (12)$$

$$\frac{\partial \Psi_0^{\text{el}}}{\partial \mathbf{R}_1^{(1)}} = \frac{\partial \tilde{\psi}_{1s}(\mathbf{r}_1^{(1)})}{\partial \mathbf{r}_1^{(1)}} \frac{\Psi_0^{\text{el}}}{\tilde{\psi}_{1s}(\mathbf{r}_1^{(1)})}, \quad (13)$$

$$\frac{\partial \Psi_0^{\text{el}}}{\partial \mathbf{R}_1} = - \left[ \frac{\partial \tilde{\psi}_{1s}(\mathbf{r}_1^{(1)})}{\partial \mathbf{r}_1^{(1)}} \frac{1}{\tilde{\psi}_{1s}(\mathbf{r}_1^{(1)})} + (\mathbf{r}_1^{(1)} \leftrightarrow \mathbf{r}_1^{(2)}) \right] \Psi_0^{\text{el}}. \quad (14)$$

Then

$$F_{fi} = F_{fi}^{\text{nuc}} + F_{fi}^{\text{el}}, \quad (15)$$

$$F_{fi}^{\text{nuc}} = \frac{i\hbar|e|N}{m_4c} \int \Psi_c^* \mathbf{A}(\mathbf{R}_1) \frac{\partial}{\partial \mathbf{R}_1} (\Psi_0^{\text{nuc}})^2 d\Omega^{\text{nuc}}, \quad (16)$$

$$\begin{aligned} F_{fi}^{\text{el}} &= - \frac{2i\hbar|e|N}{m_4c} \int \Psi_c^* (\Psi_0^{\text{el}} \Psi_0^{\text{nuc}})^2 \frac{\partial \tilde{\psi}_{1s}(\mathbf{r}_1^{(1)})}{\partial \mathbf{r}_1^{(1)}} \frac{1}{\tilde{\psi}_{1s}(\mathbf{r}_1^{(1)})} \\ &\times \left( \mathbf{A}(\mathbf{R}_1 + \mathbf{r}_1^{(1)}) \frac{m_4}{m_e} + 2\mathbf{A}(\mathbf{R}_1) \right) d\Omega^{\text{nuc}} d\Omega^{\text{el}}. \end{aligned} \quad (17)$$

### 2.1. Calculation of $F_{fi}^{\text{nuc}}$

We note that the matrix element  $F_{fi}$  in (1) is constructed on the basis of the WFs  $\Psi_i$  and  $\Psi_f$  not containing the time factor (the latter is included into the  $\delta$ -function). In formula (50\*) for  $\Psi_c$ , the coordinates of atoms can be considered as the coordinates of nuclei. Omitting the factor  $e^{-i\omega t}$ , we present  $\Psi_c$  in the form

$$\Psi_c \approx \sum_{j=1}^N \Psi_c(j), \quad \Psi_c(j) = \frac{c_{l_c, k_z, k_\rho}}{\sqrt{N}} e^{il_c \varphi_j + ik_z Z_j} J_{l_c}(k_\rho \rho_j), \quad (18)$$

below  $c_{l_c, k_z, k_\rho} \equiv \tilde{c}$ . Whence, with regard for (56\*) and (58\*), we get

$$\begin{aligned} F_{fi}^{\text{nuc}} &= \frac{i\hbar|e|N}{m_4c} \left\{ \int d\mathbf{R}_1 \Psi_c^*(1) \mathbf{A}(\mathbf{R}_1) \frac{\partial}{\partial \mathbf{R}_1} \frac{1}{V} + \right. \\ &\left. + (N-1) \int d\mathbf{R}_1 d\mathbf{R}_2 \Psi_c^*(2) \mathbf{A}(\mathbf{R}_1) \frac{\partial g(|\mathbf{R}_1 - \mathbf{R}_2|)}{V^2 \partial \mathbf{R}_1} \right\}. \end{aligned} \quad (19)$$

Since  $\frac{\partial}{\partial \mathbf{R}_1} \frac{1}{V} = 0$ , the first integral in (19) is equal to zero. As for the second integral, the integration is carried on over the region, where the helium atoms are positioned, i.e., over the region outside of the disk. Therefore, we describe the field  $\mathbf{A}$  with the use of solution (31\*)–(33\*) without the factor  $e^{-i\omega t}$  (taken into account in (5)). Denoting  $|\mathbf{R}_1 - \mathbf{R}_2| = R$ , we have

$$\mathbf{A}(\mathbf{R}_1) \frac{\partial g(R)}{\partial \mathbf{R}_1} = A_m e^{i\varphi_1} \left[ a_1(\rho_1, Z_1) \left( \frac{\partial}{\partial \rho_1} + \frac{i}{\rho_1} \frac{\partial}{\partial \varphi_1} \right) + a_2(\rho_1, Z_1) \left( -\frac{\partial}{\partial \rho_1} + \frac{i}{\rho_1} \frac{\partial}{\partial \varphi_1} \right) \right] g(R). \quad (20)$$

Using (72\*) and the relation  $\mathbf{qR}_1 = q_z Z_1 + q_\rho \rho_1 \cos(\varphi_1 - \varphi_q)$ , we obtain

$$\begin{aligned} \mathbf{A}(\mathbf{R}_1) \frac{\partial g(R)}{\partial \mathbf{R}_1} &= \frac{A_m e^{i\varphi_1}}{(2\pi)^{3n}} \int d\mathbf{q} [S(q) - 1] i q_\rho \times \\ &\times \left[ a_1(\rho_1, Z_1) e^{-i(\varphi_1 - \varphi_q)} - a_2(\rho_1, Z_1) e^{i(\varphi_1 - \varphi_q)} \right] \times \\ &\times e^{[iq_z(Z_1 - Z_2) + iq_\rho \rho_1 \cos(\varphi_1 - \varphi_q) - iq_\rho \rho_2 \cos(\varphi_2 - \varphi_q)]}, \end{aligned} \quad (21)$$

where  $n = N/V$ . In the cylindrical coordinate system,  $d\mathbf{R}_j = d\varphi_j dZ_j \rho_j d\rho_j$  and  $d\mathbf{q} = d\varphi_q dq_z q_\rho dq_\rho$ . The relation

$$J_l(x) = \frac{i^l}{2\pi} \int_{-\pi+\beta}^{\pi+\beta} e^{-ix \cos \psi \pm i l \psi} d\psi \quad (22)$$

( $\beta$  is arbitrary) yields

$$\begin{aligned} &\int_0^{2\pi} d\varphi_1 e^{[il\varphi_1 \pm i(\varphi_1 - \varphi_q) + iq_\rho \rho_1 \cos(\varphi_1 - \varphi_q)]} = \\ &= 2\pi i^{l \pm 1} e^{il\varphi_q} J_{l \pm 1}(q_\rho \rho_1), \end{aligned} \quad (23)$$

$$\begin{aligned} &\int_0^{2\pi} d\varphi_2 \exp[-il_c \varphi_2 - iq_\rho \rho_2 \cos(\varphi_2 - \varphi_q)] = \\ &= 2\pi i^{-l_c} e^{-il_c \varphi_q} J_{l_c}(q_\rho \rho_2). \end{aligned} \quad (24)$$

With regard for (32\*), (33\*), and (18), we write the required matrix element as

$$F_{fi}^{\text{nuc}} = \frac{i\delta_{l,l_c} \hbar |e| n \tilde{c} A_m}{m_4 c \sqrt{N}} \int dZ_1 dZ_2 \rho_1 d\rho_1 \rho_2 d\rho_2 dq_z \times$$

$$\begin{aligned} &\times q_\rho^2 dq_\rho J_l(q_\rho \rho_2) J_l(k_\rho \rho_2) [S(q) - 1] e^{[iq_z(Z_1 - Z_2) - ik_z Z_2]} \times \\ &\times [a_1(\rho_1, Z_1) J_{l-1}(q_\rho \rho_1) + a_2(\rho_1, Z_1) J_{l+1}(q_\rho \rho_1)]. \end{aligned} \quad (25)$$

Integrating  $\mathbf{R}_2$  over the whole volume (including the disk), we obtain

$$\begin{aligned} &\int dq_z dZ_2 e^{[iq_z(Z_1 - Z_2) - ik_z Z_2]} [S(q_z, q_\rho) - 1] = \\ &= 2\pi e^{-ik_z Z_1} [S(-k_z, q_\rho) - 1]. \end{aligned} \quad (26)$$

We pass in (25) to discrete  $q_\rho$ , by replacing  $\int dq_\rho \rightarrow \frac{\pi}{R_\infty - \tilde{R}_d} \sum_{n_\rho}$  and using the quantization conditions for  $q_\rho$  [3]:

$$k_z = \frac{2\pi n_z}{H - h_d}, \quad n_z = \pm 1, \pm 2, \dots, \quad (27)$$

$$k_\rho = \frac{\pi n_\rho}{R_\infty - \tilde{R}_d}, \quad n_\rho \gg l. \quad (28)$$

Here,  $h_d = 0.1$  cm and  $R_d = 0.95$  cm are, respectively, the height and the radius of a disk resonator, and  $H \approx 4.2$  cm and  $R_\infty \approx 2.1$  cm are the same for a chamber with helium; the numbers are indicated for the experiment [11]. The quantity  $\tilde{R}_d$  is defined in [3]: for small  $k_\rho$ ,  $\tilde{R}_d > R_d$  (in particular, for the smallest  $k_\rho$ , we have  $\tilde{R}_d \approx 1.5R_d$ ), and  $\tilde{R}_d$  decreases down to  $R_d$  with increase in  $k_\rho$ . With regard for (64\*), we will take the integral required in the calculations of (25):

$$\begin{aligned} I_p &\equiv \int \rho_2 d\rho_2 q_\rho^2 dq_\rho [S(-k_z, q_\rho) - 1] \times \\ &\times J_l(q_\rho \rho_2) J_l(k_\rho \rho_2) J_{l \pm 1}(q_\rho \rho_1) \approx \\ &\approx k_\rho [S(k) - 1] J_{l \pm 1}(k_\rho \rho_1) \frac{B(k_\rho R_\infty, l)}{1 - \tilde{R}_d/R_\infty}, \end{aligned} \quad (29)$$

$$B(x, l) = \pi x \int_0^1 y dy J_l^2(y \cdot x). \quad (30)$$

At greater  $k_\rho$ , the function  $B(k_\rho R_\infty, l) \approx 1$ , whereas it is close to 1 ( $\gtrsim 0.9$ ) at lower  $k_\rho$  ( $k_\rho R_\infty \lesssim l$ ) and can be calculated numerically.

Taking the disk into account gives  $I_p \rightarrow I_p \left( 1 - \frac{h_d}{H} \frac{R_d}{R_\infty} \frac{B(k_\rho R_d, l)}{B(k_\rho R_\infty, l)} \right)$ . Since  $h_d/H \simeq 1/42$ ,

$R_d/R_\infty \simeq 1/2$ , and  $B \approx 1$ , this consideration changes  $I_p$  only slightly, which can be neglected. From (25)–(29), we now obtain

$$F_{fi}^{\text{nuc}} = i\delta_{l,l_c}\xi\sqrt{k_\rho^3}I_{\text{nuc}}, \quad (31)$$

$$\xi = \frac{2\pi\hbar|e|n\tilde{c}A_m}{m_4c\sqrt{Nk_\rho}} \frac{B(k_\rho R_\infty, l)}{1 - \tilde{R}_d/R_\infty} [S(k) - 1], \quad (32)$$

$$I_{\text{nuc}} = \int dZ_1 \rho_1 d\rho_1 e^{-ik_z Z_1} [a_1(\rho_1, Z_1)J_{l-1}(k_\rho \rho_1) + a_2(\rho_1, Z_1)J_{l+1}(k_\rho \rho_1)]. \quad (33)$$

As is seen, we must integrate with respect to the variables  $Z_1$  and  $\rho_1$  over the region outside of the disk with regard for the distribution of the EM field calculated in [3]. We denote the values of the integral  $I_c$  taken over regions I and II from (32\*)–(33\*) by, respectively, indices 1 and 2:

$$I_{\text{nuc}} = I_{\text{nuc}}^{(1)} + I_{\text{nuc}}^{(2)}. \quad (34)$$

It will be seen below that values of the functions  $F_{fi}^{\text{nuc}}$  and  $F_{fi}^{\text{el}}$  are maximum in two limiting cases:  $k_\rho \rightarrow \infty$  and  $k_z \rightarrow \infty$ . In the first case, the simple, but sufficiently bulky calculations give

$$I_{\text{nuc}}^{(1)} \approx \frac{\cos \alpha_l(k_\rho R_d)}{k_\rho^2 \text{tg}^2 \theta_0} \sqrt{\frac{2R_d}{\pi k_\rho}} O\left(\frac{k_z + \kappa_z + Q_1 \text{tg} \theta_0}{k_\rho}\right), \quad (35)$$

$$I_{\text{nuc}}^{(2)} \approx -\frac{(2l-2)\sin \alpha_l(k_\rho R_d)}{k_\rho^2} \sqrt{\frac{2}{\pi k_\rho R_d}} I_z(k_z, R_d), \quad (36)$$

$$I_z(k_z, \rho) = \frac{J_{l-1}(Q_1 R_d) \sin\left[(\pi/\tilde{h}_d - k_z)\tilde{h}_d\right]}{\pi/\tilde{h}_d - k_z} + (k_z \rightarrow -k_z), \quad (37)$$

where  $\alpha_l(k_\rho R_d) = k_\rho R_d - \pi l/2 - \pi/4$ ,  $\tilde{h}_d = h_d/2 + (\rho - R_d)\text{ctg}\theta(\rho)$ ,  $\tilde{h}_d \approx 1.087h_d$ , and  $\theta$  is the effective angle. Using the latter, we set the line of sewing  $z(\rho)$  in (32\*), (33\*) at  $z > 0$  in the form  $\rho = R_d + (z - h_d/2)\text{tg}\theta(z)$ . The condition  $\theta_0 = \theta(z = h_d/2)$  determines this angle at the beginning of the line of sewing. In calculations,

we used the properties  $J_{l-1}(Q_1 R_d) = c_l J_{l+1}(Q_1 R_d)$  and  $n_{l-1}(Q_1^h R_d) = b_l n_{l+1}(Q_1^h R_d)$ , as well as the asymptotics of the Bessel and Neumann functions. Since  $k_z + \kappa_z + Q_1 \text{tg}\theta_0 \ll k_\rho$ , the relation  $|I_{\text{nuc}}^{(1)}| \ll |I_{\text{nuc}}^{(2)}|$  is valid.

Consider the case where  $k_z \rightarrow \infty$ . Now,  $k_\rho$  is small. The smallest  $k_\rho$  are determined by the equality  $k_\rho^{(j)} = \mu_l^{(j)}/R_d$  (see (46\*)), where  $l = l_{\text{rot}} = 66$ . Using the formulas [10]

$$\mu_l^{(1)} \approx l + 1.856l^{1/3} + 1.033l^{-1/3}, \quad (38)$$

$$\mu_l^{(2)} \approx l + 3.245l^{1/3} + 3.158l^{-1/3}, \quad (39)$$

$$\mu_l^{(3)} \approx l + 4.382l^{1/3} + 5.76l^{-1/3}, \quad (40)$$

we determine three first zeros of the Bessel function:  $\mu_{66}^{(1)} \approx 73.756$ ,  $\mu_{66}^{(2)} \approx 79.895$ , and  $\mu_{66}^{(3)} \approx 85.134$ . In order to calculate  $I_{\text{nuc}}^{(1)}$  and  $I_{\text{nuc}}^{(2)}$ , we take into account that, at small  $k_\rho$ , the component  $k_z = \sqrt{k^2 - k_\rho^2} \approx k - k_\rho^2/2k \approx k$ . Then we have

$$I_{\text{nuc}}^{(1)}(k_z \rightarrow \infty) \approx -f_{\text{nuc}}^{(1)} \frac{\sin(kh_d/2)}{4k}, \quad (41)$$

$$f_{\text{nuc}}^{(1)} = \int \rho d\rho [J_{l-1}(Q_1 \rho)J_{l-1}(k_\rho \rho) + c_l J_{l+1}(Q_1 \rho)J_{l+1}(k_\rho \rho)]. \quad (42)$$

For three smallest  $k_\rho^{(j)}$  ( $j = 1; 2; 3$ ), we determined numerically the following values:  $f_{\text{nuc}}^{(1)}/R_d^2 = 0.0023$ ,  $-0.00049$ , and  $0.00029$ . By calculating integral (33), we have

$$I_{\text{nuc}}^{(2)}(k_z \rightarrow \infty) \approx \frac{\cos\left[(\pi/\tilde{h}_d - k_z)h_d/2\right] J_{l-1}(Q_1 R_d)}{(\pi/\tilde{h}_d - k_z)^2 \text{ctg}\theta_0} \times \\ \times R_d [J_{l-1}(k_\rho R_d) + J_{l+1}(k_\rho R_d)] + (k_z \rightarrow -k_z), \quad (43)$$

which implies that  $I_{\text{nuc}}^{(2)}$  is negligible:  $|I_{\text{nuc}}^{(2)}(k_z \rightarrow \infty)| \sim |I_{\text{nuc}}^{(1)}(k_z \rightarrow \infty)|/kR_d \ll |I_{\text{nuc}}^{(1)}(k_z \rightarrow \infty)|$ .

## 2.2. Calculation of $F_{fi}^{\text{el}}$

The electron part,  $F_{fi}^{\text{el}}$ , of the total matrix element (15) can be calculated analogously. The nonzero value of  $F_{fi}^{\text{el}}$  is determined by the difference

$$\mathbf{A}(\mathbf{R} + \mathbf{r}) - \mathbf{A}(\mathbf{R}) = \mathbf{e}_\varphi(\mathbf{R}) \cdot \left(\frac{\partial A_\varphi}{\partial \mathbf{R}} \mathbf{r}\right) +$$

$$\begin{aligned}
& + \mathbf{e}_\rho(\mathbf{R}) \cdot \left( \frac{\partial A_\rho}{\partial \mathbf{R}} \mathbf{r} \right) - \mathbf{A}(\mathbf{R}) \frac{y \sin \varphi + x \cos \varphi}{\rho} + \\
& + A_\varphi \frac{-y \mathbf{i} + x \mathbf{j}}{\rho} + A_\rho \frac{x \mathbf{i} + y \mathbf{j}}{\rho} + O(r^2), \quad (44)
\end{aligned}$$

where  $\mathbf{R} = (\rho \cos \varphi, \rho \sin \varphi, Z)$ ,  $\mathbf{r} = (x, y, z)$ , and we took into account that, as  $R$  is much more than the atom size ( $R \gg r$ ),

$$\mathbf{e}_\varphi(\mathbf{R} + \mathbf{r}) \approx \mathbf{e}_\varphi(\mathbf{R}) \left( 1 - \frac{y \sin \varphi + x \cos \varphi}{\rho} \right) - \frac{y}{\rho} \mathbf{i} + \frac{x}{\rho} \mathbf{j}, \quad (45)$$

$$\mathbf{e}_\rho(\mathbf{R} + \mathbf{r}) \approx \mathbf{e}_\rho(\mathbf{R}) \left( 1 - \frac{y \sin \varphi + x \cos \varphi}{\rho} \right) + \frac{x}{\rho} \mathbf{i} + \frac{y}{\rho} \mathbf{j}. \quad (46)$$

Representing  $\mathbf{A}$  in the form

$$\mathbf{A} = A_\rho(\rho, \varphi, Z) \mathbf{e}_\rho + A_\varphi(\rho, \varphi, Z) \mathbf{e}_\varphi, \quad (47)$$

we obtain

$$F_{fi}^{\text{el}} = \frac{i\hbar|e|\tilde{n}\tilde{c}}{m_e c \sqrt{N}} (I_1 + I_2), \quad (48)$$

$$\begin{aligned}
I_1 &= \int d\mathbf{R} e^{-il_c \varphi - ik_z Z} J_l(k_\rho \rho) \times \\
&\times [A_\rho + \partial A_\varphi / \partial \varphi + \rho \partial A_\rho / \partial \rho] / \rho, \quad (49)
\end{aligned}$$

$$\begin{aligned}
I_2 &= n \int d\mathbf{R}_1 d\mathbf{R}_2 g(\mathbf{R}_1 - \mathbf{R}_2) e^{-il_c \varphi_2 - ik_z Z_2} \times \\
&\times \frac{J_l(k_\rho \rho_2)}{\rho_1} \left[ A_\rho(\mathbf{R}_1) + \frac{\partial A_\varphi(\mathbf{R}_1)}{\partial \varphi_1} + \frac{\rho_1 \partial A_\rho(\mathbf{R}_1)}{\partial \rho_1} \right]. \quad (50)
\end{aligned}$$

Using relations (72\*), (22)–(30), we can verify that

$$I_2 \approx I_1 [S(k) - 1] \frac{B(k_\rho R_\infty, l)}{1 - \tilde{R}_d / R_\infty}, \quad (51)$$

$$I_1 = 2\pi A_m \delta_{l,c} I_{\text{el}}, \quad (52)$$

$$I_{\text{el}} = \int dZ d\rho J_l(k_\rho \rho) e^{-ik_z Z} \{ (1-l)a_1(\rho, Z) -$$

$$- (1+l)a_2(\rho, Z) + \rho \partial / \partial \rho (a_1(\rho, Z) - a_2(\rho, Z)) \}, \quad (53)$$

where the integration is carried on over the volume occupied by helium. Analogously to (34), we divide  $I_{\text{el}}$  into the sum of integrals over regions I and II. Then we have

$$I_{\text{el}} = I_{\text{el}}^{(1)} + I_{\text{el}}^{(2)}, \quad (54)$$

$$I_{\text{el}}^{(1)} = \left( \int_{-\infty}^{-h_d/2} + \int_{h_d/2}^{\infty} \right) \frac{dZ}{8} e^{-ik_z Z - \kappa_z (|Z| - h_d/2)} I_{\text{el},\rho}^{(1)}(Z), \quad (55)$$

$$\begin{aligned}
I_{\text{el},\rho}^{(1)}(Z) &= \int_0^{\check{R}_d} d\rho J_l(k_\rho \rho) [(1-l)J_{l-1}(Q_1 \rho) - \\
&- (1+l)c_l J_{l+1}(Q_1 \rho) + Q_1 \rho J'_{l-1}(Q_1 \rho) - \\
&- c_l Q_1 \rho J'_{l+1}(Q_1 \rho)], \quad (56)
\end{aligned}$$

$$\begin{aligned}
I_{\text{el}}^{(2)} &= \int_{R_d}^{\infty} d\rho I_z(k_z, \rho) J_l(k_\rho \rho) [(1-l)n_{l-1}(Q_1^h \rho) - \\
&- (1+l)b_l n_{l+1}(Q_1^h \rho) + \\
&+ Q_1^h \rho n'_{l-1}(Q_1^h \rho) - b_l Q_1^h \rho n'_{l+1}(Q_1^h \rho)], \quad (57)
\end{aligned}$$

where  $I_z(k_z, \rho)$  is defined above,  $\check{R}_d = R_d + (|Z| - h_d/2) \text{tg} \theta(Z)$ ,  $J'_l(x) = \partial J_l(x) / \partial x$ , and  $n'_l(x) = \partial n_l(x) / \partial x$ . The integrals  $I_{\text{el}}^{(1)}$  and  $I_{\text{el}}^{(2)}$  are calculated analogously to  $I_{\text{nuc}}^{(1)}$  and  $I_{\text{nuc}}^{(2)}$ . Eventually, we get

$$\begin{aligned}
I_{\text{el}}^{(1)}(k_\rho \rightarrow \infty) &\approx - \frac{l J_{l-1}(Q_1 R_d)}{2k_\rho^2 \text{tg} \theta_0} \sqrt{\frac{2}{\pi k_\rho R_d}} \times \\
&\times \cos \alpha_l(k_\rho R_d) \cos(k_z h_d/2) \left\{ 1 - \frac{Q_1 R_d}{2l J_{l-1}(Q_1 R_d)} \times \right. \\
&\times [J'_{l-1}(Q_1 R_d) - c_l Q_1 \rho J'_{l+1}(Q_1 R_d)] \left. \right\}, \quad (58)
\end{aligned}$$

$$I_{\text{el}}^{(2)}(k_\rho \rightarrow \infty) \approx \frac{2l-2}{k_\rho} \sqrt{\frac{2}{\pi k_\rho R_d}} \sin \alpha_l(k_\rho R_d) \times$$

$$\times I_z(k_z, R_d) = -k_\rho I_{\text{nuc}}^{(2)}(k_\rho \rightarrow \infty). \quad (59)$$

At  $k \gg 1/h_d$ , the integral  $I_{\text{el}}^{(1)}$  is negligible:  $|I_{\text{el}}^{(1)}| \sim |I_{\text{el}}^{(2)}|/k_\rho h_d \ll |I_{\text{el}}^{(2)}|$ . Formulas (35) and (58) do not involve the condition  $\Psi_c = 0$  for the disk surface. For its consideration, we need to make replacements  $\cos(k_z h_d/2) \rightarrow \sin(k_z h_d/2)$ ,  $\cos \alpha_l(k_\rho R_d) \rightarrow \sin \alpha_l(k_\rho R_d)/k_\rho R_d \approx 1/k_\rho R_d \ll 1$  in the formulas, which decreases  $I_{\text{nuc}}^{(1)}$  and  $I_{\text{el}}^{(1)}$  still further.

At small  $k_\rho$ , we obtain

$$I_{\text{el}}^{(1)}(k_z \rightarrow \infty) \approx -f_{\text{el}}^{(1)} \frac{\sin(k h_d/2)}{4k}, \quad (60)$$

$$f_{\text{el}}^{(1)} = \int_0^{R_d} d\rho J_l(k_\rho \rho) [(1-l)J_{l-1}(Q_1 \rho) - (1+l)c_l J_{l+1}(Q_1 \rho) + Q_1 \rho J'_{l-1}(Q_1 \rho) - c_l Q_1 \rho J'_{l+1}(Q_1 \rho)]. \quad (61)$$

For  $k_\rho^{(j)}$  with  $j = 1; 2; 3$ , we get numerically:  $f_{\text{el}}^{(1)}/R_d = -0.17, 0.039$ , and  $-0.025$ . In addition,

$$I_{\text{el}}^{(2)}(k_z \rightarrow \infty) \approx \frac{\cos[(\pi/\tilde{h}_d - k_z)h_d/2]}{(\pi/\tilde{h}_d - k_z)^2 \text{ctg}\theta_0} \times J_{l-1}(Q_1 R_d) J_l(k_\rho R_d) \times \{(1-l)n_{l-1}(Q_1^h R_d) - (1+l)b_l n_{l+1}(Q_1^h R_d) + Q_1^h R_d [J'_{l-1}(Q_1^h R_d) - b_l J'_{l+1}(Q_1^h R_d)]\} + (k_z \rightarrow -k_z) \sim \frac{I_{\text{el}}^{(1)}(k_z \rightarrow \infty)}{k R_d} \ll I_{\text{el}}^{(1)}(k_z \rightarrow \infty). \quad (62)$$

With regard for (31), (32), (48)–(52), the performed calculations allow us to write finally

$$F_{fi}^{\text{el}} = \delta_{l,l_c} b(k_\rho, l) \xi \sqrt{k_\rho} I_{\text{el}}, \quad (63)$$

$$b(k_\rho, l) = \frac{m_4}{m_e} \left( \frac{1 - \tilde{R}_d/R_\infty}{[S(k) - 1]B(k_\rho R_\infty, l)} + 1 \right). \quad (64)$$

### 2.3. Total matrix transition element $F_{fi}$

We have

$$F_{fi} = F_{fi}^{\text{el}} + F_{fi}^{\text{nuc}} \approx \delta_{l,l_c} \xi \sqrt{k_\rho} [k_\rho I_{\text{nuc}} + b(k_\rho, l) I_{\text{el}}], \quad (65)$$

whence the total probability of the creation of a c-phonon with “momentum”  $k$  is

$$w_{fi} = \sum_{l_c, n_z, n_\rho} \delta w_{fi} = \frac{2\pi}{\hbar} \sum_{l_c, n_z, n_\rho} |F_{fi}|^2 \delta(E_f - E_i^{(0)} - \hbar\omega) = \frac{2\pi}{\hbar} \sum_{n_z, n_\rho} |\xi|^2 k_\rho [k_\rho I_{\text{nuc}} + b(k_\rho, l) I_{\text{el}}]^2 \delta(E_c(k) - \hbar\omega). \quad (66)$$

Moreover,  $k^2 = k_\rho^2 + k_z^2$  in all formulas. The main contribution to sum (66) is given by the regions ( $k_z \rightarrow 0$ ,  $k_\rho \rightarrow k$ ) and ( $k_\rho \rightarrow 0$ ,  $k_z \rightarrow k$ ). We now determine these contributions.

a) Region of small  $k_z$  (here,  $k_\rho \rightarrow k$ ). According to (34)–(37) and (54), (58), (59), we have  $I_{\text{nuc}}(k_\rho \rightarrow \infty) \approx I_{\text{nuc}}^{(2)}(k_\rho \rightarrow \infty)$ ,  $I_{\text{el}}(k_\rho \rightarrow \infty) \approx I_{\text{el}}^{(2)}(k_\rho \rightarrow \infty)$ . In (66), we now pass from the sum  $\sum_{n_\rho}$  to the integral  $\sum_{n_\rho} \rightarrow \frac{R_\infty - R_d}{\pi} \int dk_\rho$  and then, with the help of the relation  $k dk = k_\rho dk_\rho$ , to an integral over  $k$ . Due to the  $\delta$ -function, this integral is easily calculated. After some transformations, we obtain

$$w_{fi}(k_z \rightarrow 0) = S_1 \frac{2b_0^2 |\xi_0|^2 h_d^2 (R_\infty - R_d)}{R_d \hbar k^2 \partial E / \partial k}, \quad (67)$$

$$S_1(k) = \frac{8(l-1)^2}{\pi h_d^2} \sum_{n_z} \frac{k^3}{k_\rho^3} \sin^2 \alpha_l(k_\rho R_d) I_z^2(k_z, R_d) \approx (2/\pi) [(l-1)J_{l-1}(Q_1 R_d) \sin \alpha_l(k R_d)]^2 \times \sum_{n_z} \left\{ \frac{\sin(\frac{\pi h_d}{2h_d} - n_z \frac{\pi h_d}{H-h_d})}{\frac{\pi h_d}{2h_d} - n_z \frac{\pi h_d}{H-h_d}} + (k_z \rightarrow -k_z) \right\}^2 \approx \frac{4.3(H-h_d)}{\pi h_d} [(l-1)J_{l-1}(Q_1 R_d) \sin \alpha_l(k R_d)]^2, \quad (68)$$

where  $n_z = \pm 1, \pm 2, \dots$ ,  $b_0 = b(B = 1, \tilde{R}_d = R_d) = \frac{m_d}{m_e} \frac{S(k) - R_d/R_\infty}{S(k) - 1}$ ,  $\xi_0 = \xi(B = 1, \tilde{R}_d = R_d)$ , and the value of  $k$  is determined from the condition  $E_c(k) \equiv E(k) = \hbar\omega$ . For  $k_z$ , we used the quantization laws (27), which assumes the zero boundary conditions on the container walls.

b) Region of small  $k_\rho$ . With the use of  $k_z = \frac{2\pi n_z}{H - h_d}$  (see (27)) and  $k_\rho^{(j)} = \mu_l^{(j)}/R_d$ , relations (34), (41)–(43), (54), (60)–(62) yield

$$\sum_{n_z} f(k) \delta(E(k) - \hbar\omega) = \frac{H - h_d}{2\pi} \int_{-\infty}^{\infty} dk_z f(k) \times \times \delta(E(k) - \hbar\omega) = \frac{H - h_d}{\pi} \frac{k}{k_z} \frac{f(k)}{\partial E/\partial k}, \quad (69)$$

$$w_{fi}(k_\rho \rightarrow 0) = S_2 \frac{2(H - h_d)R_d b_0^2 |\xi_0|^2}{\hbar k^2 \partial E/\partial k}, \quad (70)$$

$$S_2(k) = \sum_{j=1, \dots} \frac{k}{k_z} \frac{k_\rho^{(j)}}{R_d} \frac{1 - f}{1 - f_j} \times \times \left| \frac{S(k) - f}{S(k) - 1 + B^{-1}(k_\rho^{(j)} R_\infty, l)(1 - f_j)} \right| \times \times \left\{ \frac{k_\rho^{(j)} k I_{\text{nuc}}(k_\rho^{(j)})}{b_0} + k I_{\text{el}}(k_\rho^{(j)}) \right\} \times \times \left. \frac{S(k) - 1 + (1 - f_j)B^{-1}(k_\rho^{(j)} R_\infty, l)}{S(k) - f} \right\}^2 \equiv \equiv a(k, l) \sin^2 \left( \frac{k h_d}{2} \right). \quad (71)$$

where  $f = R_d/R_\infty$ ,  $f_j = \tilde{R}_d(k_\rho^{(j)})/R_\infty$ .

Formulas (68) and (71) include  $\sin \alpha_l(kR_d)$  and  $\sin(kh_d/2)$ . Due to the zero boundary conditions,  $\sin \alpha_l(k_\rho R_d) \approx \pm 1$ , whence  $\sin \alpha_l(kR_d) \approx \pm 1$ . In view of the same conditions, we set  $\sin(kh_d/2) \approx \pm 1$ .

Using (31), (32), (75\*), and the formula for the volume of helium  $V = \pi R_\infty^2 H$ , we obtain finally:

$$w_{fi} \approx w_{fi}(k_z \rightarrow 0) + w_{fi}(k_\rho \rightarrow 0) \approx$$

$$\approx \frac{2\pi^2(1 - h_d/H)n\hbar(eA_m)^2|S(k) - f|}{c^2 k^2 m_e^2 \partial E/\partial k} \times \times \left( \frac{8.6h_d}{\pi R_d} [(l - 1)J_{l-1}(Q_1 R_d)]^2 + \frac{2f a(k, l)}{1 - f} \right). \quad (72)$$

We note that the main contribution to  $w_{fi}(k_\rho \rightarrow 0)$  and  $w_{fi}(k_z \rightarrow 0)$  is given by the electron part of  $F_{fi}$ , and the transition probability  $w_{fi}$  is determined by the quantities  $w_{fi}(k_z \rightarrow 0)$  and  $w_{fi}(k_\rho \rightarrow 0)$ , i.e., by the creation of c-phonons with the smallest  $k_z$  and large  $k_\rho$  and with the smallest  $k_\rho$  and large  $k_z$  (almost plane c-phonons). We now evaluate these contributions quantitatively for the roton line and conditions of the experiment [1, 2]. According to [3], the relation  $J_{l-1}(Q_1 R_d) \approx 1/27.831$  is valid at  $l = l_{\text{rot}} = 66$ . To calculate  $a(k, l)$  in (71), we use the roton value  $S(k) \approx 1.3$  (for  $T \lesssim 1.4 K$ ). Moreover, we consider that the relation  $k_z/k \approx 1$  holds as  $k_\rho \rightarrow 0$ ,  $\tilde{R}_d \approx 1.5R_d$  at  $j = 1$  [3], and the quantity  $R_d$  decreases down to  $R_d$  with increase in  $j$ . We calculated values of  $B(k_\rho R_\infty, l = 66)$  numerically by formula (30):  $B(k_\rho^{(1)} R_\infty, 66) \approx 0.91$ ,  $B(k_\rho^{(2)} R_\infty, 66) \approx 0.93$ , and  $B(k_\rho^{(3)} R_\infty, 66) \approx 0.94$ . The contribution of the following  $k_\rho$  (with  $j > 3$ ) to  $a(k, l)$  is small. Whence we find  $a(k_{\text{rot}}, l) \approx 0.2$ . Moreover, since  $B \approx 1$ , the functions  $a(k, l)$  and  $S_2$  are almost independent of  $k$ . But if  $k$  are such that  $S(k) \rightarrow f$ , then the coefficient  $a(k, l)$  increases by several orders of magnitude, approximately as  $|S(k) - f|^{-1}$ , and becomes  $\gg 0.2$ . But, for the probability  $w_{fi}$ , such a growth is canceled by the factor  $|S(k) - f|$  in (72) in front of the large parentheses.

Using these numbers, the relation  $R_\infty \approx H/2 \approx 2.1$  cm, and (71), we obtain that the probability of the creation of c-phonons with large  $k_\rho$  is  $\sim 5$  times more than that for the almost plane ones (with small  $k_\rho$ ). Thus, a resonator creates c-phonons mainly of two “extreme” types: almost completely circular and almost plane. The high probability of the creation of c-phonons with an almost plane structure is a somewhat unexpected result. At the same time, it is clear that the completely plane phonons cannot be created due to the angular momentum conservation law: a phonon must possess a certain “twist” ( $l \neq 0$ ,  $k_\rho \neq 0$ ) in order to carry away the angular momentum of a c-photon.

### 3. Width of the Roton Absorption Line

As was mentioned above, the spectrum of the SHF emission of a disk resonator contains the very narrow absorption line at the roton frequency ( $\hbar\omega = \Delta_{\text{rot}} = 8.65 K k_B$ ).

Let the line width be the distance between the points, which are located on both sides from the line center, and for which the intensity of a signal is about 0.8 of the background one (the signal far from the line). Then it follows from the experiment [1, 2] that the line width is about 50 kHz at  $T = 1.8$  K and decreases, at lower  $T$ , to the resolving power of a spectroscope ( $\simeq 30$  kHz). Moreover, the width stops to decrease at  $T \lesssim 1.6$  K and approaches a constant  $\simeq 30$  kHz. The minimum experimental temperature  $T = 1.4$  K, but formula (72) is applicable, if there are no c-rotors in the initial state of helium, i.e., at  $T = 0$ . Because the width does not depend on  $T$  already at  $T \lesssim 1.6$  K, we may assume that the width at  $T = 0$  is the same as that at  $T = 1.4$  K.

The creation of a c-phonon (or a c-roton) is caused by the c-photon  $\rightarrow$  c-phonon transition. In order to calculate its probability, we should divide  $w_{fi}$  (72) by the number of c-photons in a resonator,  $N_{\text{phot}}$ . We can calculate the latter by dividing the total energy of the EM field of the resonator,

$$W = \int dV \frac{\mathbf{DE} + \mathbf{BH}}{8\pi} = \int dV \frac{\varepsilon_{\perp} \dot{\mathbf{A}}^2 / c^2 + (\text{rot} \mathbf{A})^2}{8\pi}, \quad (73)$$

by the energy of a c-photon,  $\hbar\omega$ . Since the field outside of the disk is weak, we will consider only the field inside the disk determined by formulas (17\*) and (18\*). Since

$$\int_0^{R_d} \rho d\rho J_{l-1}^2(Q_1 \rho) \approx \frac{R_d^2}{2} \left[ J_{l-1}'(\mu_{l-1}^{(1)}) \right]^2 \approx 2 \times 10^{-3} R_d^2 \quad (74)$$

and  $\cos(\pi h_d / 2\tilde{h}_d) = 1/8$ , we obtain

$$W \approx 10^{-3} A_m^2 R_d^2 h_d \left[ \left( \frac{\varepsilon_{\perp} \omega^2}{c^2} + \frac{Q_1^2}{2} \right) \left( 1 + \frac{\tilde{h}_d}{4\pi h_d} \right) + \frac{\pi^2}{\tilde{h}_d^2} \left( 1 - \frac{\tilde{h}_d}{4\pi h_d} \right) \right], \quad (75)$$

where the small terms contributing to  $W$  are omitted. Using (75), it is easy to evaluate the total energy and the number of c-photons in the pumping band ( $\Delta\nu_{\text{pump}} \simeq 50$  kHz) for the roton mode ( $l = 66$ ) and at the roton frequency:

$$W \approx 9.2 A_m^2 h_d (R_d / 0.95 \text{ cm})^2 \approx 3.87 \times 10^8 \text{ eV}, \quad (76)$$

$$N_{\text{phot}} = \frac{W}{\hbar\omega} \approx 5.19 \times 10^{11}. \quad (77)$$

In a vicinity of the roton minimum, we have  $\partial E(k) / \partial k = \hbar^2 |k - k_{\text{rot}}| / m_{\text{rot}}$  with  $m_{\text{rot}} \approx 0.165 m_4$ ,  $k_{\text{rot}} = 1.93 \text{ \AA}^{-1}$ . Then the probability  $\tilde{w}_{fi} = w_{fi} / N_{\text{phot}}$  of the c-photon  $\rightarrow$  c-roton process for the experimental width  $\Delta\nu = 30$  kHz is

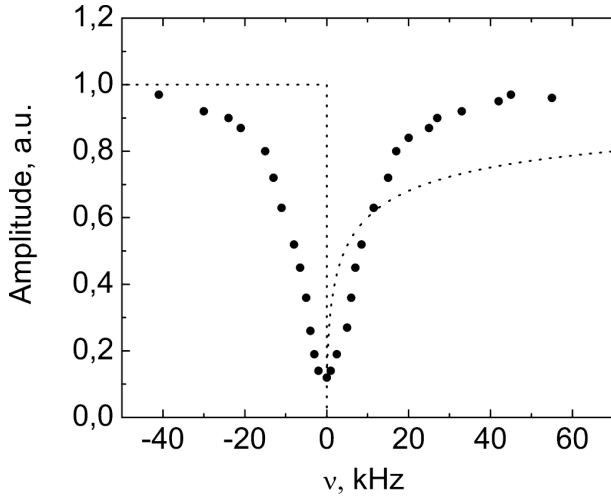
$$\begin{aligned} \tilde{w}_{fi} &\approx \frac{4\pi^2}{9.2} \frac{(1 - h_d/H) n e^2 \omega m_{\text{rot}} |S(k) - f|}{m_e^2 k^2 c^2 h_d |k - k_{\text{rot}}|} \times \\ &\times \left( \frac{4.3 h_d}{\pi R_d} [(l-1) J_{l-1}(Q_1 R_d)]^2 + \frac{f a(k, l)}{1-f} \right) \times \\ &\times \left( \frac{0.95 \text{ cm}}{R_d} \right)^2 \approx 3.36 \times 10^{-7} \omega_{\text{rot}}. \end{aligned} \quad (78)$$

This process weakens the flow of photons propagating from the resonator. We now determine the absorption line width. To this end, we consider properties of the resonator. In the experiment [11], the pumping signal with the frequency band  $\Delta\nu_{\text{pump}}$  and the power  $w_{\text{pump}}^0 \simeq 10^{-3}$  W was firstly switched-on. But, as a result of losses, the resonator received  $w_{\text{pump}} \simeq 10^{-4} \div 10^{-5}$  W. The resonator accumulates and amplifies the pumping signal, but, in this case, the energy losses in the resonator increase also, until a stationary equilibrium state is established. In this state, the losses in the resonator due to the emission are equal to the pumping. In other words, the condition of equilibrium for the EM field of the resonator with frequencies in the pumping band is the equality of the pumping energy flow and the losses:

$$w_{\text{pump}} = N_{\text{phot}} \hbar\omega / \tau_{\text{ren}}. \quad (79)$$

Here,  $N_{\text{phot}}$  and  $\tau_{\text{ren}}$  are, respectively, the number of c-photons in the resonator and the mean emission time of a c-photon by the resonator (obviously, it is also the period of renewal of EM modes of the resonator). By the value of  $w_{\text{pump}}$ , we can estimate the electrical signal formed by an antenna catching photons emitted by the resonator as  $w \simeq 4 \times 10^{-8}$  W. It follows from the distribution of the stationary EM field of the resonator [3] that this field induces the signal  $w \lesssim 4 \times 10^{-21}$  W in the antenna which is weaker by 13 orders. In other words, the signal generated by the antenna is due to photons emitted by the resonator, rather than to the stationary EM field of the latter.

When the frequency of the EM field approaches the roton one, then, according to (78), the probability of the emission of c-rotors by the resonator becomes large. We now consider the frequency interval  $\Delta\nu_0 =$



Intensity of the signal received by the antenna *vs* the frequency near a narrow roton absorption line,  $T = 1.63$  K.  $\bullet\bullet$  — experiment [1], dotted line — theory (by the present work). The frequency is equal to that indicated in the figure plus 175.7 GHz (this number is the roton energy at  $T = 1.63$  K)

$\Delta\nu_{\text{pump}}/100 \simeq 0.5$  kHz, which is much less than the line width and the pumping band, but it contains a macroscopic number of quanta. If the emission of c-rotors occurs, then the condition of equilibrium for the band  $\Delta\nu_0$  takes the form

$$0.01w_{\text{pump}} = 0.01N_{\text{phot}}\hbar\omega/\tau_{\text{ren}} + N_{\text{rot}}^0\Delta_{\text{rot}}/\tau_{\text{em}}, \quad (80)$$

where  $\tau_{\text{em}} = 1/\tilde{w}_{fi}$  is a duration of the emission of a c-roton by a c-photon of the resonator, and  $N_{\text{rot}}^0$  is the number of c-rotors emitted for a time interval  $\tau_{\text{em}}$  by c-photons from the band  $\Delta\nu_0$ . In this case, the losses of the resonator are separated into the channels of emission of c-photons and c-rotors. Respectively, the flow of emitted c-photons decreases, which is manifested in the resonator spectrum as the absorption. As was mentioned above, the signal is equal to 80% of the background one on the edge of lines. Hence, 20% of the losses of the resonator are transferred into c-rotors, whereas 80% pass into c-photons. Thus, each c-photon of the resonator in the frequency band  $\Delta\nu_0$  for the time  $\tau_{\text{ren}}$  emits a c-photon with a probability of 0.8 and a c-roton with a probability of 0.2. This yields  $\tau_{\text{em}} = 4\tau_{\text{ren}}$ , which allows us to write the following condition for the line edge:

$$\tilde{w}_{fi} \equiv \frac{1}{\tau_{\text{em}}} = \frac{1}{4\tau_{\text{ren}}}. \quad (81)$$

Relations (77), (79) yield  $\tau_{\text{ren}} \simeq 6.25(10^{-7} \div 10^{-6})$  s, which corresponds to the experimental value  $\tau_{\text{ren}} \simeq 10^{-6}$  s. Using the last value of  $\tau_{\text{ren}}$  and (81), we obtain

$\tilde{w}_{fi}$  for the line edge:  $\tilde{w}_{fi} = 1/4\tau_{\text{ren}} \simeq 2.5 \times 10^5 \text{ s}^{-1} \approx 2.2 \times 10^{-7}\omega_{\text{rot}}$ , which is only by a factor of 1.5 less than the theoretical value of  $\tilde{w}_{fi}$  (78).

The theoretical and experimental lines are shown in Figure. At  $\nu > \nu_{\text{rot}}$ , the amplitude of the former is given by the formula  $a \approx \left(1 + \sqrt{\frac{4.4kH\lambda}{\nu - \nu_{\text{rot}}}}\right)^{-1}$ . In this case, the error of the line width is about one order; it is related to the approximate character of the solutions for the WF of a c-phonon (not completely correct consideration of boundary conditions) and for the EM field of the resonator, as well as to the neglect of a deviation of a symmetry of the system far from the disk (antenna, container's wall, *etc.*) from the cylindrical symmetry. As is seen from Figure, the theoretical line corresponds approximately to the experimental one by width, but does not by shape. The density of states  $\varrho(E) = \int \delta(E(k) - \hbar\omega) d\mathbf{k} = \frac{4\pi k^2}{\partial E/\partial k}$  is high in the region above the energy  $\Delta_{\text{rot}}$  of a roton ( $\varrho(E) = \frac{4\pi k^2 m_{\text{rot}}}{\hbar^2 |k - k_{\text{rot}}|} \rightarrow \infty$  at  $k \rightarrow k_{\text{rot}}$ ). Below  $\Delta_{\text{rot}}$ , no roton states are present, and the density of states decreases sharply to a value corresponding to the linear phonon curve:  $\varrho(E) = \frac{4\pi k^2}{u_1 \hbar}$ . Therefore, for the c-photon  $\rightarrow$  c-roton transition, the line must sharply fall on the side of lower frequencies, whereas the experimental line is almost symmetric. This difference means that the process is more complicated and involves at least two particles, rather than one particle (c-photon  $\rightarrow$  c-roton), as was accepted above. In particular, one more c-phonon can be created, or a part of the angular momentum of a c-photon can be absorbed by the disk. We hope to clarify the mechanism in the future investigations.

It is necessary also to take into account that a spreading of the c-roton energy due to the interaction between quasiparticles can also contribute to the line width. However, this leads to a very large line width of the order of magnitude of the width  $\sim 0.1\Delta_{\text{rot}}$  in neutron experiments. This value is larger by 6 orders than the width of the narrow SHF line and by 4 orders than the mode width. Therefore, this spreading cannot be observed for a single mode, but it is revealed as a "pedestal" (base) on many modes [2].

The number of photons approaching the receiver is diminished not only due to the creation of c-rotors by the field of the resonator, but also due to their creation by c-photons already emitted by the resonator. The time-of-flight of these photons to the receiver is  $\sim 4\lambda/c_h \approx 3 \times 10^{-11} \text{ s} \simeq 10^{-5}\tau_{\text{em}}$ , which is less by 5 orders than the duration of the emission of a c-roton by a photon of the resonator. In this case, the probabilities

of the emission of a c-roton for a standing photon of the resonator and a running photon are of the same order, because a standing c-photon is simply a superposition of two radial c-photons propagating toward each other. Therefore, the line is formed not due to the absorption of running photons, but, as we have assumed, due to the absorption of “standing” photons of the resonator.

#### 4. Discussion

While calculating formula (78), we used the solution for the EM field [3], for which the sewing in the corner region ( $|z| \geq h_d/2, \rho = R_d \div \infty$ ) is approximate. In this region, the EM field is weak. But, nevertheless, it influences the value of  $\tilde{w}_{fi}$ . To evaluate this effect, we calculated the probability  $\tilde{w}_{fi}$  for two other distributions of the EM field in the corner region:  $\mathbf{A}_h = 0$  and  $\mathbf{A}_h = A_m e^{i(l\varphi - \omega t)} [a_1(\rho, z)(\mathbf{e}_\rho + i\mathbf{e}_\varphi) + a_2(\rho, z)(-\mathbf{e}_\rho + i\mathbf{e}_\varphi)]$ ,  $\{a_1(\rho, z), a_2(\rho, z)\} = \frac{1}{8} J_{l-1}(Q_1 R_d) e^{-\kappa_z(|z| - h_d/2)} \times \{n_{l-1}(Q_1^h \rho), b_l n_{l+1}(Q_1^h \rho)\}$ . The latter can be sewed with solutions in other regions, but it does not completely satisfy the equation. Moreover, if we use  $Q_1$  instead of  $Q_1^h$ , then the equation is satisfied, but the sewing cannot be executed. The value of  $\tilde{w}_{fi}$  for such solutions differs from (78) by several times; therefore,  $\tilde{w}_{fi}$  is not very sensitive to the sewing. The analysis indicates that it is of importance to correctly set the solution in the corner region near the joint with adjacent regions, and it is not so important in bulk. Solution (32\*), (33\*) satisfies this condition, so that its use is justified.

As was mentioned above, probability (78) of the c-photon  $\rightarrow$  c-roton process grows strongly at  $\partial E(k)/\partial k \rightarrow 0$ , i.e., near the points of an extremum of the dispersion curve  $E(k)$ . This peculiarity explains why the narrow line is observed namely at the roton frequency and predicts the possibility to find one more line at the frequency of the maxon maximum,  $\nu_{\max} \approx 287 \pm 2$  GHz [12] (up to now, the frequencies  $\nu \approx 40 \div 200$  GHz were studied). Let us substitute the maxon parameters ( $k_{\max} = 1.12 \text{ \AA}^{-1}$ ,  $m_{\max} \approx 0.54m_4$ ,  $S(k) \approx 0.3$ ) in (78), and let us take into account that, in the denominator, the number  $9.2 \sim \omega^2$ , and, according to (19\*) and (20\*), it should be  $l \sim \omega$  for the resonance mode. We obtain  $\tilde{w}_{fi} \approx 5.9 \times 10^{-7} \omega_{\max}$ . Thus, without regard for an additional factor (see above), we have that if  $\tau_{\text{ren}}$  is approximately identical for the maxon and roton lines, then the width of the maxon line must be larger by a factor of 1.7 (at  $T = 0$ ) than the width of the roton line.

The peculiarity at  $\partial E(k)/\partial k \rightarrow 0$  is well known in solid-state physics as the Van Hove singularity. At  $|\partial E(\mathbf{k})/\partial \mathbf{k}| \rightarrow 0$ , the states of c-rotions falling in the small given energy interval are strongly concentrated. Respectively, the transition probability in this energy interval sharply increases. In crystals, the narrow lines of light absorption [13] and neutron scattering [14] were registered a lot of times. However, the width of the latter is larger by several orders than those of SHF lines in helium and corresponds to the pedestal. Thus, the narrow SHF line in helium is related to the Van Hove singularity, like the lines of crystals, but its widening is caused by another mechanism.

In neutron experiments with liquid helium, the analogous very narrow peaks must be observed on the scattering curve  $S(k = \text{const}, \omega)$  at the frequencies of the roton and maxon extrema. However, the high error of neutron measurements ( $\delta\omega \approx 0.1$  K) does not allow one to register these peaks.

In addition to the processes considered above, one more channel is possible: c-photon  $\rightarrow$  p-phonon + the transfer of a momentum to the disk and the transfer of an angular momentum to the disk or for the creation of a vortex rotating around the disk. Such processes must be less probable, since the greater the number of quasiparticles participating in a process, the less is the probability of the process. Moreover, what is more important, the overlapping of the wave functions of the EM field and a p-phonon is insignificant due to different symmetries.

In order to explain the appearance of the narrow line of absorption, the authors of work [2] proposed to consider the following process: p-photon  $\rightarrow$  p-roton + the transfer of a momentum to helium as a whole. In our opinion, the transfer of a momentum to the disk can be more probable in such an approach, since the disk is a tougher system as compared with helium. The approach with a plane photon and a plane phonon is the main alternative to the above-considered process with c-rotions. But the latter is, apparently, more probable by two reasons.

1) As was mentioned above, the line is formed by the stationary EM field of the resonator, rather than by running photons. The EM field outside of the resonator can be represented as a superposition of plane waves (wave packets). But the total EM field of the resonator is a sum of c-photons localized outside and inside the disk (see [3]). At the creation of a c-roton, a c-photon disappears *as a whole* inside and outside of the disk. But, due to different values of  $\varepsilon$  of helium and the disk, such a c-photon cannot be presented in the form of a superposition of photons which are plane in both helium and

the disk (a photon is not plane or in helium, or in the disk). In other words, we must be based in the input equations on the *circular* field of the resonator. In addition, the properties of this field are unlike those of plane waves, because the field of the resonator sharply drops with increase in the distance to the resonator.

2) In addition, the approach with p-photons requires the expansion of the field in multipoles. Here, the main contribution is given by the term with the dipole moment (DM)  $\mathbf{d}_0$  of a roton. It was assumed in work [2] that such a stationary DM arises in a roton due to the mutual polarization of atoms, and the probability of the p-photon  $\rightarrow$  p-phonon transition is proportional to  $d_0$ . It was also proposed in [15] that a vortex ring possesses an intrinsic DM. However, both quasiparticles create the reciprocal motion of atoms: a part of atoms moves forward, but the similar part moves backward. In this case, the separated direction is set by the velocity of a quasiparticle. Therefore, the appearance of a DM is related to the asymmetry of a quasiparticle relative to the forward-backward directions. The question about the presence of such an asymmetry can be clarified with the help of the following reasoning (which belongs to Yu. V. Shtanov). By definition, the stationary DM of a quasiparticle is equal to

$$\mathbf{d}_{qp} = \int d\mathbf{R}_1 d\mathbf{R}_1^{(1)} d\mathbf{R}_1^{(2)} \dots d\mathbf{R}_N d\mathbf{R}_N^{(1)} d\mathbf{R}_N^{(2)} \Psi_{qp}^* \Psi_{qp} \times \\ \times e(\mathbf{R}_1^{(1)} + \mathbf{R}_1^{(2)} - 2\mathbf{R}_1 \dots + \mathbf{R}_N^{(1)} + \mathbf{R}_N^{(2)} - 2\mathbf{R}_N), \quad (82)$$

where  $\Psi_{qp} = \Psi_{qp}(\mathbf{R}_1, \mathbf{R}_1^{(1)}, \mathbf{R}_1^{(2)}, \dots, \mathbf{R}_N, \mathbf{R}_N^{(1)}, \mathbf{R}_N^{(2)})$  is the WF of a quasiparticle. Let us make inversion of time  $t \rightarrow -t$ . In this case, we have  $\Psi \rightarrow \Psi^*$  [5], and DM (82) is not changed. But the DM must be directed along the velocity of a quasiparticle, i.e., it should change the sign. This implies that the DM is zero. It was considered in [15] that, by the CPT-theorem, the charges also change their signs at  $t \rightarrow -t$ , which gives  $\mathbf{d}_{qp} \neq 0$ . However, the change  $t \rightarrow -t$  in the equation can be performed formally without any connection with the time arrow. Then the charges conserve their signs at  $t \rightarrow -t$ , and the DM turns out zero.

The real quasiparticle is a wave pocket, but it is clear that, in this case,  $\mathbf{d}_{qp} = 0$  as well.

Such a consideration is not valid if the state of a quasiparticle is degenerate. In other words, at given  $E$  and  $\mathbf{k}$ , there are the states with DMs  $\mathbf{d}_{qp}$  and  $-\mathbf{d}_{qp}$  which can transit to each other at  $t \rightarrow -t$ . However, we have no reasons to consider that a roton or a ring has such a degeneration. For  $\mathbf{d}_{qp} \neq 0$ , there appears another possibility, if

the reflected state is unstable and transits in a stable one with the inverse DM. This internal irreversibility can be related to the ordering of deformations of the electron shells of atoms induced by the interaction with neighbors. For clearness, we note that this is similar to a flag on a moving car. Such a flag points out always the direction opposite to one of the motion. At  $t \rightarrow -t$ , we obtain a flag indicating the direction of motion, i.e., we obtain the unstable state. A similar structure of a ring or a roton is possible in principle. But it is improbable, especially for a roton representing reciprocal oscillations of the density. It is of importance that such a change of the symmetry, like that at  $t \rightarrow -t$ , will happen at the reflection of a quasiparticle from the wall. At each reflection, the quasiparticle must loss energy. Hence, it will be unstable. Such an instability is possible for rings, and it could explain why the rings are not discovered in the spectrum of quasiparticles or by the contribution to the heat capacity till now. But such an instability seems impossible for phonons and rotons. Thus, a roton has no stationary DM. This is also the case for a ring, most probably. This reasoning implies that, while explaining the narrow line, the circular symmetry of the problem must be taken into account already in the input equations.

## 5. The Line Spectrum of Liquid $^4\text{He}$

As is known from the general theorems of quantum mechanics, a many-particle system located in a finite volume possesses a discrete energy spectrum. Liquid  $^4\text{He}$  in a vessel is a system of this kind. The energy levels of He II can be determined from the WF of He II calculated for the zero boundary conditions. From here, it is obvious that the real energy spectrum of He II is not a Landau continuous curve, but it is a collection of separate disconnected points very densely lying on this curve. According to (27), (28), the observed roton line [1, 2] consists of  $\sim 10^5$  individual roton lines. If the experiment will be executed with a film of helium  $\sim 100 \text{ \AA}$  in thickness, the distances between lines increases by 6 orders of magnitude, and they will become resolvable. In this case, instead of a single roton line, we will measure many lines in the wide range of the frequencies:  $\nu = 0 \div 2\Delta_{\text{rot}}/2\pi\hbar$ . Thus, it will be possible to observe, for the first time, the line spectrum of a fluid consisting of a huge number of discrete lines, like the spectrum of an atom. It is only necessary that the intensities of lines be sufficiently high. However, if the resonator disk is only covered by a helium film, no lines will be observed. Indeed, by (72), the intensities of lines will be of

the same order of magnitude as those for a thick layer of helium [1, 2]. But the line registered for such a layer consists of  $\sim 10^5$  individual lines which are too weak to be observed separately. To resolve them, one needs to increase their intensity by 4-5 orders of magnitude. This is a task for future studies.

## 6. Quantization of the Amplitude of the Roton Line

The experiment [16] revealed one more unusual effect: as the power  $\dot{Q}$  of a heat gun increases, the amplitude  $A_R$  of the roton absorption peak decreases, and this occurs stepwise. This fact testifies to the “quantization” of the roton line amplitude. It was noted in [16] that this effect can be related to the quantization of the azimuth velocity  $\mathbf{v}_s$  (around the resonator), but the nature of this connection is not clear yet. Since the growth of  $A_R$  means a decrease in the number of c-rotors created by SHF-photons, we assume that each step of  $A_R$  means a decrease in the number of created c-rotors by some integer.

In He II near the resonator, two competing processes occur: c-photons create c-rotors and *vice versa*. In this case, a c-roton can transit only in a c-photon with the same energy and the same  $l$ . From the state  $|N_{\text{phot}}, N_{\text{rot}}\rangle$  with  $N_{\text{phot}}$  c-photons and  $N_{\text{rot}}$  c-rotors, the transition in two following states is possible: *i*) the state  $|N_{\text{phot}} + 1, N_{\text{rot}} - 1\rangle$ , if a c-roton creates a c-photon; *ii*) the state  $|N_{\text{phot}} - 1, N_{\text{rot}} + 1\rangle$ , if a c-photon creates a c-roton.

Since circular photons and rotors are bosons, we can associate the creation operators with them. Within the formalism of secondary quantization for bosons, we obtain the transition probability (*i*)

$$w(\text{rot} \mapsto \text{phot}) = G(N_{\text{phot}} + 1)N_{\text{rot}}. \quad (83)$$

For (*ii*), we have

$$w(\text{phot} \mapsto \text{rot}) = G(N_{\text{rot}} + 1)N_{\text{phot}}, \quad (84)$$

whence

$$\begin{aligned} \Delta w &\equiv w(\text{rot} \mapsto \text{phot}) - w(\text{phot} \mapsto \text{rot}) = \\ &= G(N_{\text{rot}} - N_{\text{phot}}), \end{aligned} \quad (85)$$

where  $G = w(\text{phot} \mapsto \text{rot})$  at  $N_{\text{phot}} = 1, N_{\text{rot}} = 0$ . In other words,  $G$  is the above-calculated probability (78) of the c-photon  $\rightarrow$  c-roton transition in the case where there is a single c-photon in the initial state of the system, and there are no c-rotors. If  $\Delta w < 0$ , then the roton line in

the spectrum of an SHF signal is a line of absorption of photons; but if  $\Delta w > 0$ , the roton line is a line of their emission (“maser” effect). In the experiment, the absorption line becomes weaker, as the power of a heat gun increases, and transits to the emission line at  $\dot{Q} = \dot{Q}_c \approx 0.5 \text{ W/cm}^2$ . We assume that these facts are related to the forced creation of c-rotors by a gun. Though all details of the mechanism are unclear up to now, we indicate several points.

a) A gun is directed along a tangent to the disk, i.e., so that the transfer of an angular momentum should be maximum. The p-rotors have no angular momentum, but the c-rotors have ( $L_z = \hbar l_c$ ). Therefore, their creation is accompanied by the transfer of both the energy and the angular momentum. It was noticed in [16] that a step of  $\dot{Q}$  corresponds to an increase in  $v_s$  on the output of a gun by a value coinciding with the quantum  $\hbar/m_4 R_d$  of a circular velocity of helium near the resonator, according to the formula  $v_s^\varphi = n_c \hbar/m_4 R_d$ . The maximum experimental number of steps was  $n_c^{\text{max}} \sim 3 \times 10^5$ . Such a quantization of the velocity can mean that a gun creates a vortex in the superfluid component near the disk, whose axis coincides with the disk axis, and each step corresponds to the increase of the circulation by 1. On the other hand, the action of the operator of azimuth momentum  $-\frac{i\hbar\partial}{\rho_j\partial\varphi_j}$  on the factor  $e^{il\varphi_j}$  of the WF of a c-roton gives  $\hbar l/\rho_j$ . Dividing it by the  $^4\text{He}$  atom mass, we obtain the azimuth velocity  $v_\varphi = \hbar l/m_4 \rho_j$ . Thus, a c-roton induces the quantized rotation of helium atoms around the resonator with the velocity  $v_\varphi = \hbar l/m_4 \rho$ , like a vortex. But this rotation is accompanied by simultaneous oscillations. In turn, an increase in the circular velocity of helium  $v_\varphi$  by an external factor must stimulate the creation of c-phonons (including c-rotors). Apparently, a gun creates a macroscopic vortex in helium (or a superposition of vortices) and many plane and circular phonons and rotors, so that the ensemble of quasiparticles near the disk is quite complicated. Moreover, some processes (e.g., decays) are allowed for c-phonons and forbidden for p-phonons.

b) The results of experiments with a gun testify unambiguously that an EM wave creates namely c-, rather than p-rotors. If the latter would be created, then a decrease in the amplitude of the roton absorption line would be related, according to (85), only to that a gun increases their number. But it increases also at a simple increase in the temperature (without switching-on a gun); however, the measurements show that this does not cause a weakening of the roton line and its transition into an emission line.

c) In a disk resonator, “left” (L) and “right” (R) c-photons differing by the sign of  $l$  are created. A waveguide captures the total signal from the resonator, i.e., the summary field of L- and R-waves. In this case, the amplitude of one of these waves in the resonator is  $\sim 100$  times greater than another one [11]. However, a gun creates c-rotons with only a single polarization, L- or R-, which depends on the position of a gun. Since an L c-photon can induce only an L c-roton (the same is true, respectively, for right ones), Eq. (85) should be written separately for L- and R-quanta. Then we obtain that the summary absorption line disappears if the relation  $N_{\text{rot}} = N_{\text{phot}}$  holds true for the dominant photon mode. A gun is able to weaken the line if the signs of  $l$  for a c-roton and the dominant c-photon coincide and cannot weaken if the signs do not coincide. Thus, let a gun weaken the line at a given configuration of the EM field. But if a gun is reoriented so that it twists He II in the opposite direction, it must stop to weaken the line. It seems to us that this assertion can be easily verified in experiments.

## 7. Stark Effect

Finally, we mention the observation of the linear Stark effect in helium-II — the roton absorption line splits into two lines in a constant electric field  $\mathbf{E}_0$  directed in the disk plane. The distance between them increases  $\sim E_0$  [17]. In [18, 19], the authors advanced the idea of the relation of the effect to a possible quadrupole or instantaneous dipole, respectively, moment of a p-roton. We agree that a p-roton as a wave packet can possess an instantaneous DM  $\mathbf{d}_{\text{rot}}$  with fluctuating (or pulsing) value and direction. This DM is due to, in particular, the interaction of the roton with neighboring quasiparticles located nonuniformly. Such a DM induces an addition  $\sim \mathbf{d}_{\text{rot}}\mathbf{E}_0$  to the roton energy. Since the projection of  $\mathbf{d}_{\text{rot}}$  on  $\mathbf{E}_0$  takes the values in the continuous band  $[-\bar{d}_{\text{rot}}^z E_0, \bar{d}_{\text{rot}}^z E_0]$ , the mentioned addition transforms the roton level to the band. However, experiments demonstrate the splitting of the line into two ones, rather than a single band. Thus, the instantaneous DM of a roton cannot explain the observed line splitting.

According to quantum mechanics, the effect can be explained if the roton energy level possesses at least a twofold degeneration which is taken off by the field  $\mathbf{E}_0$ . In our opinion, the effect is determined by the existence of right ( $l = l_{\text{rot}}$ ) and left ( $l = -l_{\text{rot}}$ ) c-rotons with the same energy, whose superposition is described by the wave function  $C_1\psi_{\text{rot}}^{\text{cir}}(l) + C_2\psi_{\text{rot}}^{\text{cir}}(-l)$ . Since a perturbing potential is obviously proportional to the applied

field  $\mathbf{E}_0$ , we obtain the splitting of a twofold degenerate energy level which is proportional to  $E_0$ . It can be evaluated by the well-known formulas of perturbation theory for a degenerate state. The field  $\mathbf{E}_0$  induces the polarization of the dielectric resonator, which is directed along  $\mathbf{E}_0$ , and takes off the degeneration, by breaking the circular symmetry. But the multiple degeneration by  $k_z$  remains (several tens of small  $k_z$  significantly contribute to the line). So, if the field  $\mathbf{E}_0$  will be directed along the  $Z$  axis, then the line must be split into two lines due to the removal of the degeneration relative to a change in the sign of  $k_z$ .

At the switching-on of a heat gun, we may expect the following. In the field  $\mathbf{E}_0$ , the eigenfunctions of the Hamiltonian of He II are not the  $R$ - and  $L$ -functions,  $\psi_{\text{rot}}^{\text{cir}}(l)$  and  $\psi_{\text{rot}}^{\text{cir}}(-l)$ , but their superpositions  $\psi_{\text{rot}}^{\text{cir}}(l) \pm \psi_{\text{rot}}^{\text{cir}}(-l)$  characteristic of a twofold degenerate level [20]. The gun oriented along a tangent to the disk creates the quantized rotation of helium in a *single* direction and increases the number of c-rotons with one ( $R$  or  $L$ ) polarization. It is obvious that, in this case, the gun cannot excite the states  $\psi_{\text{rot}}^{\text{cir}}(l) \pm \psi_{\text{rot}}^{\text{cir}}(-l)$  ( $R \pm L$ -superposition of two c-rotons with the counter rotation). Therefore, if the field  $\mathbf{E}_0$  was already switched-on (earlier than the gun), the gun will not decrease the peaks of the split roton line and will not induce the maser effect. It would be of interest to verify this prediction in experiments in similar fashion.

## 8. Conclusion

It is seen from the above-presented analysis that the experiment [1, 2] has revealed the existence of particular excitations in He II — circular rotons which are azimuth sound waves. In the present work, we have approximately calculated the probability of the creation of a circular roton by the EM field of the resonator and, on its basis, have evaluated the width of the absorption line at the roton frequency. The theoretical line is close to the experimental one by width but differs by shape.

We have also advanced the assumption that the splitting of the line into two ones in a constant electric field is caused by the presence of right and left c-rotons and, respectively, by the twofold degeneration of the energy level of a circular roton.

The authors are grateful to V.N. Derkach, E.Ya. Rudavskii, and A.S. Rybalko for numerous discussions of the experiment and to Yu.V. Shtanov for valuable remarks and advices.

1. A. Rybalko, S. Rubets, E. Rudavskii, V. Tikhii, S. Tarapov, R. Golovashchenko, and V. Derkach, *Phys. Rev. B* **76**, 140503(R) (2007).
2. A.S. Rybalko, S.P. Rubets, E.Ya. Rudavskii, V.A. Tikhii, Yu.M. Poluektov, R.V. Golovashchenko, V.N. Derkach, S.I. Tarapov, and O.V. Usatenko, *Low Temp. Phys.* **35**, 837 (2009).
3. V.M. Loktev and M.D. Tomchenko, *Ukr. J. Phys.* **55**, 901 (2010).
4. V.M. Loktev and M.D. Tomchenko, *Phys. Rev. B* **82**, 172501 (2010).
5. L.D. Landau, E.M. Lifshitz, *Quantum Mechanics. Non-Relativistic Theory* (Pergamon, New York, 1980).
6. V.B. Berestetskii, E.M. Lifshitz, and L.P. Pitaevskii, *Relativistic Quantum Theory* (Pergamon Press, Oxford, 1982).
7. W. Byers Brown and D.M. Whisnant, *Mol. Phys.* **25**, 1385, **26**, 1105 (1973).
8. V.M. Loktev and M.D. Tomchenko, *J. Phys. B: At. Mol. Opt. Phys.* **44**, 035006 (2011); *Rep. Nat. Acad. Sciences Ukr.* No. 5, 76 (2010) (in Russian).
9. M.D. Tomchenko, arXiv:cond-mat/1003.4389 v3 (2010).
10. E. Janke, F. Emde, F. Lösch, *Tafeln Höherer Funktionen* (Teubner, Stuttgart, 1960).
11. A.S. Rybalko, private communication.
12. M.R. Gibbs, K.H. Andersen, W.G. Stirling, H. Schober, *J. Phys. Cond. Mat.* **11**, 603 (1999).
13. A.S. Davydov, *Theory of Molecular Excitons* (Plenum, New York, 1971).
14. D. Pines, *Elementary Excitations in Solids* (Benjamin, New York, 1963).
15. V.M. Loktev and M.D. Tomchenko, *Low Temp. Phys.* **34**, 262 (2008).
16. A.S. Rybalko, S.P. Rubets, E.Ya. Rudavskii, V.A. Tikhii, R.V. Golovashchenko, V.N. Derkach, S.I. Tarapov, *Low Temp. Phys.* **34**, 254 (2008).
17. A.S. Rybalko, S.P. Rubets, E.Ya. Rudavskii *et al.*, arXiv:cond-mat/0807.4810 (2008).
18. L.A. Melnikovsky, cond-mat/0808.1188 (2008).
19. V.P. Mineev, *JETP Lett.* **90**, 866 (2009).
20. I.O. Vakarchuk, *Quantum Mechanics* (L'viv National University, L'viv, 2004) (in Ukrainian).

Received 25.10.10

## ДО ПРИРОДИ ВУЗЬКОЇ РОТОННОЇ ЛІНІЇ ПОГЛИНАННЯ В СПЕКТРІ ДИСКОВОГО НВЧ РЕЗОНАТОРА

В.М. Локтев, М.Д. Томченко

## Резюме

Обчислено імовірність народження “круговим” фотоном (к-фотоном) резонатора к-фонона в He II. Показано, що вона має різкий максимум на частотах, за яких ефективна група швидкості фонона обертається на нуль та густина станів сильно зростає. Для He II такі частоти відповідають ротону і максону. На основі імовірності народження к-ротона знайдено ширину ротонної лінії, яка наближено узгоджується з експериментальною. Зроблено висновок, що спостережувана в надвисокочастотному (НВЧ) спектрі поглинання гелію-II ротонна лінія пов'язана з народженням кругових ротонів. Запропонована також можлива інтерпретація ефекта Штарка, який спостерігався для ротонної лінії.